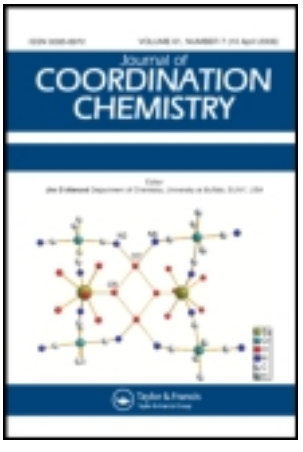

Journal of Coordination Chemistry
Publication details, including instructions for authors and subscription information:
http://www.tandfonline.com/loi/gcoo20

A Schiff-base porphyrin complex with double intramolecular hydrogen bonds

Wei Huang [a], Jiaxun Jiang [a], Zhiqiang Feng [a], Xiaoxu Kai [a], Chuanjiang Hu [a b], Hong Yu [a] & Wen Yang [a]

[a] Key Laboratory of Organic Synthesis of Jiangsu Province, College of Chemistry, Chemical Engineering and Materials Science, Soochow University, Suzhou 215123, P.R. China

[b] State Key Lab & Coordination Chemistry Institute, Nanjing University, Nanjing 210093, P.R. China

Published online: 13 Jun 2011.

To cite this article: Wei Huang, Jiaxun Jiang, Zhiqiang Feng, Xiaoxu Kai, Chuanjiang Hu, Hong Yu & Wen Yang (2011) A Schiff-base porphyrin complex with double intramolecular hydrogen bonds, Journal of Coordination Chemistry, 64:12, 2101-2109, DOI: 10.1080/00958972.2011.589002

To link to this article: http://dx.doi.org/10.1080/00958972.2011.589002

Journal of Coordination Chemistry
Vol. 64, No. 12, 20 June 2011, 2101–2109

A Schiff-base porphyrin complex with double intramolecular hydrogen bonds

WEI HUANG†, JIAXUN JIANG†, ZHIQIANG FENG†, XIAOXU KAI†, CHUANJIANG HU*†‡, HONG YU† and WEN YANG†

†Key Laboratory of Organic Synthesis of Jiangsu Province, College of Chemistry, Chemical Engineering and Materials Science, Soochow University, Suzhou 215123, P.R. China
‡State Key Lab & Coordination Chemistry Institute, Nanjing University, Nanjing 210093, P.R. China

(*Received 1 March 2011; in final form 22 April 2011*)

We have designed a porphyrin with a Schiff-base substituent as a model to study intramolecular hydrogen-bonding. The corresponding complex [Zn(SATPP)(CH_3OH)] has been synthesized and characterized by X-ray crystallography, ^{1}H NMR, and UV-Vis spectroscopy. The structure shows that there are three phenyl groups and one salicylideneaminophenyl group at the meso positions of the porphyrin, and the phenol oxygen is involved in double hydrogen bonds, one within the salicylideneaminophenyl and the other between coordinated methanol and phenol oxygen. ^{1}H NMR spectra suggest that the binding of methanol to zinc is an equilibrium process in solution and the equilibrium constant has been determined by UV-Vis measurements. The intramolecular hydrogen bond stabilizes the structure, and the binding affinity increases 10 times over the corresponding TPP (TPP, dianion of meso-5,10,15,20-tetraphenylporphyrin).

Keywords: Porphyrin; Intramolecular hydrogen bond; Schiff base; Salicylideneaminophenyl; Binding constant

1. Introduction

Hydrogen bonds are common interactions in biological system and can be used to control the microenvironment around metal ions. They are found in heme proteins, such as myoglobin, cytochrome P450, and horseradish peroxidase. There has been substantial speculation that hydrogen-bonding in heme proteins could control the relative stability of the oxidation state of iron and even control the reactivity of the heme protein [1]. For example, in myoglobin, the hydrogen-bonding interactions involving the distal histidine can stabilize the iron-bound oxygen [2]. In cytochrome P-450cam, the crystallographic structure reported by Poulos *et al.* [3] suggested the presence of weak double NH $\cdots$ S hydrogen bonds between S of Cys 357 and two amide NHs of Gly 359 and Gln 360, which are accompanied by a positive shift of the reported redox potential [4]. In horseradish peroxidase [5, 6], the proximal histidine (His170) forms a strong hydrogen bond with a highly conserved aspartate group Asp247.

*Corresponding author. Email: cjhu@suda.edu.cn

ISSN 0095-8972 print/ISSN 1029-0389 online © 2011 Taylor & Francis
DOI: 10.1080/00958972.2011.589002

It has been postulated that this hydrogen bond increases the basicity of the His170 proximal ligand, thus helping to stabilize high oxidation state intermediates [6].

We recently studied the effect of hydrogen-bonding on the molecular and electronic structure in iron porphyrins [7]. Our ongoing interest is to develop porphyrin complexes having intramolecular hydrogen bond(s). Since Collman's group developed picket-fence porphyrins [8], *o*-aminophenyl-substituted porphyrins have been used as a building block to develop various model compounds. However, most are amide derivatives and the corresponding Schiff-base derivatives have not been reported. Herein, we design a Schiff-base porphyrin as shown in scheme 1. Different from the amide derivatives which favor the "exo" conformation [9], due to the intramolecular hydrogen-bonding between O and N, the designed porphyrin will favor the "endo" conformation with the phenol OH facing the porphyrin ring. Such rigid structure makes phenol capable of forming another hydrogen bond with the coordinated ligand. Different from most hydrogen-bonding models, such hydrogen bond is directly related to the coordinated atom. Therefore, it could be a good model to study the effect of hydrogen-bonding on ligand-binding affinity in porphyrin complexes. In this article, we have synthesized a zinc complex of the designed porphyrin, [Zn(SATPP)(CH_3OH)] (SATPP, dianion of 5-(2-salicylideneaminophenyl)-10,15,20-triphenylporphyrin) and characterized it by ^1H NMR and X-ray crystallography. The binding constant of zinc to methanol has been determined by UV-Vis measurements.

2. Experimental

2.1. *General procedures*

2.1.1. Materials and general methods. Dichloromethane was fresh distilled. All reagents were analytical grade and used without purification. [Zn(ATPP)] (ATPP, dianion of 5-(2-aminophenyl)-10,15,20-triphenylporphyrin) was prepared according to literature procedure [10]. All solvents were used as received. ^1H NMR spectra were carried out using a Bruker AVANCE 400 spectrometer.

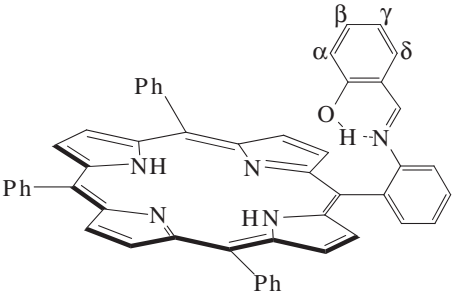

Scheme 1. A Schiff-base porphyrin with an intramolecular hydrogen bond which makes the phenol OH face the porphyrin ring to form an "endo" conformation.

2.2. *Synthesis of [Zn(SATPP)(CH$_3$OH)]*

Salicylaldehyde (2.0 mL, 19.1 mmol) was added to a solution of [Zn(ATPP)] (0.69 g, 1.0 mmol) in chloroform (200 mL). The mixture was refluxed overnight. The solvent was reduced to about 2 mL, filtered, and washed with absolute ethanol to give a light purple solid. It was recrystallized in the mixture of methylene chloride and hexane. Yield 0.44 g (55%). Anal. Calcd for $C_{51}H_{33}N_5OZn \cdot 0.5CH_2Cl_2$ (%): C, 73.66; H, 4.08; N, 8.34. Found (%): C, 73.84; H, 4.23; N, 8.73. X-ray quality crystals were obtained by liquid diffusion of methanol into toluene solution in 8 mm diameter glass tubes.

2.3. *X-ray crystallography*

X-ray data collection was made on a Rigaku Mercury CCD X-ray diffractometer by using graphite-monochromated Mo-Kα ($\lambda = 0.071073$ nm) at 223(2) K. The structure was solved by direct methods and refined on F^2 using full-matrix least-squares methods with SHELXTL version 97 [11]. Anisotropic thermal parameters were refined for non-hydrogen atoms. Two hydrogens, H(2o) and H(5n), were found in Fourier maps, their coordinates and isotropic temperature factors were refined, other hydrogens were theoretically added and riding on their parent atoms. Toluene was disordered over two positions and both were refined as rigid groups. After the final refinement the occupancy of the major orientation was found to be 64%. Brief crystal data for both structures are listed in table 1.

2.4. *Equilibrium constant determination*

UV-Vis spectra were measured on a Shimadzu UV-3150 spectrometer. Microliter amounts of freshly distilled methanol were added to a 5.0×10^{-5} mol L^{-1} [Zn(SATPP)] in freshly distilled CH_2Cl_2. The concentrations of methanol for UV-Vis measurements range from 2.27×10^{-3} to 9.88×10^{-2} mol L^{-1}. Absorbance changes were monitored by observing the increase in intensity of the Q band at 557 nm.

3. Results and discussion

3.1. *Molecular structure*

The designed porphyrin complex has been synthesized by Schiff-base condensation of [Zn(ATPP)] with excess salicylaldehyde in refluxing chloroform. The solid formed was further crystallized in a mixture of toluene and methanol to give X-ray quality crystals of $[Zn(SATPP)(CH_3OH)] \cdot C_6H_5CH_3$.

The crystal structure of $[Zn(SATPP)(CH_3OH)] \cdot C_6H_5CH_3$ has been solved in the $P2(1)/n$ space group, and one asymmetric unit consists of one zinc porphyrinate and one interstitial toluene molecule. The ORTEP diagram of porphyrin is presented in figure 1. There are three phenyl groups and one salicylideneaminophenyl group at meso positions. Zinc is five-coordinate with methanol as the axial ligand. The corresponding distance Zn(1)–O(2) is 2.187(3) Å; other related distances are also listed in table 2. These Zn–O and Zn–N distances are similar to the corresponding distances in

Table 1. Crystallographic data for $[Zn(SATPP)(CH_3OH)] \cdot C_6H_5CH_3$.

Formula	$C_{59}H_{45}N_5O_2Zn$
Formula weight	921.37
Temperature (K)	223(2)
Crystal system	Monoclinic
Space group	$P2(1)/n$
Unit cell dimensions (Å, °)	
a	10.862(2)
b	38.497(8)
c	12.016(2)
α	90
β	111.90(3)
γ	90
Volume (Å^3), Z	4661.9(16), 4
Calculated density, ρ_{calc} (g cm^{-3})	1.313
μ (mm^{-1})	0.577
$F(000)$	1920
Reflections collected	23,178
Unique reflections	8150 [R(int) = 0.0750]
Parameters	655
Goodness of fit	1.109
R_1 [$I > 2\sigma(I)$]	0.0714
wR_2 (all data)	0.1277

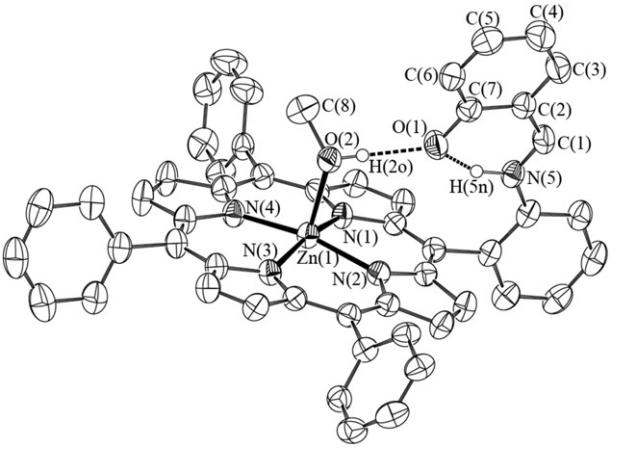

Figure 1. ORTEP view for $[Zn(SATPP)(CH_3OH)]$ at 50% probability thermal ellipsoids. The hydrogens except H(2o) and H(5n) have been omitted for clarity.

Table 2. Selected bond lengths (Å) and angles (°) for $[Zn(SATPP)(CH_3OH)] \cdot C_6H_5CH_3$.

Zn(1)–N(1)	2.061(3)	Zn(1)–N(2)	2.057(3)
Zn(1)–N(3)	2.064(3)	Zn(1)–N(4)	2.059(3)
Zn(1)–O(2)	2.187(3)	C(1)–N(5)	1.298(5)
C(1)–C(2)	1.417(6)	C(2)–C(3)	1.411(6)
C(3)–C(4)	1.359(6)	C(4)–C(5)	1.384(6)
C(5)–C(6)	1.372(6)	C(6)–C(7)	1.393(6)
C(2)–C(7)	1.425(6)	C(7)–O(1)	1.331(5)
C(8)–O(2)	1.436(5)	–	–

Table 3. Hydrogen bond lengths (Å) and angles (°) for $[Zn(SATPP)(CH_3OH)] \cdot C_6H_5CH_3$.

D–H···A	*d*(D–H)	*d*(H···A)	*d*(D···A)	∠(DHA)
O(2)–H(2o)···O(1)	0.83(5)	1.85(5)	2.676(4)	179(5)
N(5)–H(5n)···O(1)	0.99(6)	1.63(6)	2.534(5)	150(5)

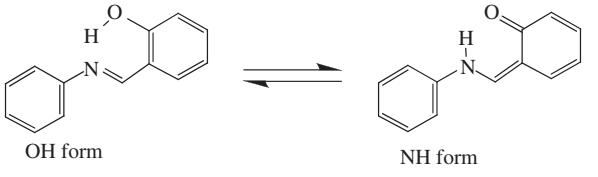

Scheme 2. The tautomeric equilibrium between the OH and NH forms in salicylideneaminophenyl.

$[Zn(TPP)(CH_3OH)]$ [12] and $[Zn(OEDPP)(CH_3OH)]$ [13] (OEDPP, dianion of 2,3,7,8,12,13,17,18-octaethyl-5,10-diphenylporphyrin).

The most interesting feature is the intramolecular hydrogen bonds in this molecule. As expected from our design, there are two intramolecular hydrogen bonds. Related distances and angles are listed in table 3. One hydrogen bond is between phenol oxygen and imine nitrogen in the salicylideneaminophenyl group. The corresponding N(5)···O(1) distance is 2.534(5) Å. N(5), H(5n), O(1), C(7), C(2), and C(1) form a six-membered ring, which stabilizes the "endo" conformation. To our surprise, the crystal structure reveals that corresponding hydrogen H(5n) is located near imine nitrogen N(5) with N(5)–H(5n) distance as 0.99(6) Å, and O(1) is actually in essence deprotonated by the proximate imine N(5), which corresponds to the NH form as shown in scheme 2. Such NH form has also been observed in the solid state of N-(5-chloro-2-hydroxybenzylidene)-4-hydroxyaniline [14]. In these salicylideneaniline species, a tautomeric equilibrium occurs between the OH and NH forms as shown in scheme 2 [15]. However, the resonance of phenol OH in ^{1}H NMR spectra indicates that OH form is dominant in solution. So the above studies suggest that salicylideneaminophenyl group in $[Zn(SATPP)(CH_3OH)]$ adopts different forms in solution and solid state: the OH form dominates in solution while in solid state, the tautomeric equilibrium is strongly shifted to the NH form. Similar cases have also been found in the recent study by Makal *et al*. [16].

Besides the intramolecular hydrogen bond in the salicylideneaminophenyl group, the other one is between coordinated methanol oxygen and phenol oxygen. The distance from O(2) to O(1) is 2.676(4) Å, and the corresponding angle of O(2)–H(2o)···O(1) is 179(5)°, which indicates a strong hydrogen bond. Phenol oxygen plays a role as a double acceptor in both hydrogen bonds. The structure suggests salicylideneaminophenyl is a suitable substituent for intramolecular hydrogen-bonding studies.

3.2. *Spectral studies*

The hydrogen-bonding effect on ligand binding has also been studied by ^{1}H NMR and UV-Vis spectroscopy. Due to the ring current effect, chemical shifts provide a

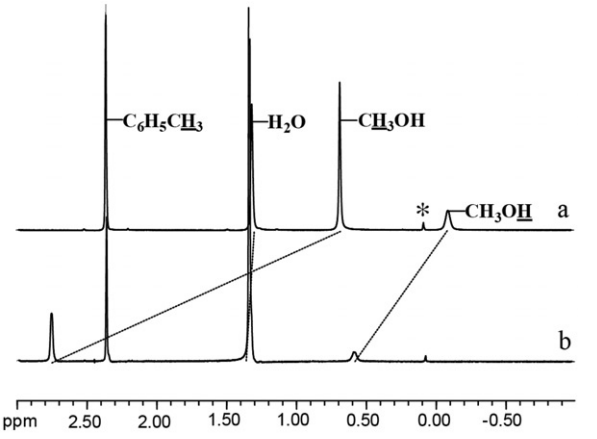

Figure 2. ^{1}H NMR spectra of $[Zn(SATPP)(CH_3OH)]\cdot C_6H_5CH_3$ in the selected region in $CDCl_3$: (a) concentrated solution and (b) diluted solution. *Impurity from silicone grease.

very useful probe of intramolecular interactions [17]. The ^{1}H NMR spectra of $[Zn(SATPP)(CH_3OH)]\cdot C_6H_5CH_3$ in the selected region in $CDCl_3$ are shown in figure 2. The binding of methanol to zinc and the "endo" conformation are verified by ^{1}H NMR studies in solution. Since protons above the porphyrin plane are in the shielded region, the ring current effect causes a remarkable upfield shift when methanol is coordinated to zinc. Such shift is evidenced by resonances of methanol proton at 0.68 and −0.09 ppm as shown in figure 2(a). Compared with free methanol, these resonances shift upfield by 2.81 and 1.18 ppm, respectively. Notably, there is another signal at 1.31 ppm, which is believed to be resonance of water protons. In $CDCl_3$, H_2O is a common impurity which usually has a resonance at 1.56 ppm. However, such resonance also shifts upfield by 0.25 ppm, which suggests that part of water is also coordinated to zinc in solution. Thus two equilibria are involved as shown in scheme 3. The resonances observed are average contributions from both coordinated and uncoordinated CH_3OH (or H_2O). These equilibria are further confirmed by the concentration-dependent ^{1}H NMR spectra. The spectrum of the diluted solution is shown in figure 2(b). The resonances of methanol shift significantly downfield to 2.75 and 0.58 ppm. It can be rationalized as the following: the equilibrium (1) will be driven to the reverse reaction when the concentrations of both reactants decrease; it will eventually increase the ratio of uncoordinated to coordinated methanol, which causes the corresponding proton resonances to shift downfield. At the same time, the resonance of water in the diluted solution also shifts downfield to 1.33 ppm. The ratio of uncoordinated to coordinated water increases as the amount of uncoordinated H_2O increases, which causes the average H_2O resonance to shift downfield.

Besides the significant shifts of methanol resonances, other protons over the porphyrin plane also show some upfield shifts. The resonances of four arene protons (α, β, γ, and δ) are located at 5.37, 6.50, 6.60, and 7.07 ppm (figure S1), which are consistent with the "endo" conformation as shown in scheme 1. The resonance of the hydroxyl proton is located at 12.27 ppm, similar to 13.27 ppm for the corresponding proton in salicylideneanilines. Such resonance is consistent with intramolecular hydrogen-bonding, otherwise the OH proton will be in the more effective shielding region than those arene protons, which will cause more upfield shift.

$$[\text{Zn (SATPP)}] + CH_3OH \overset{K}{\rightleftharpoons} [\text{Zn (SATPP)}(CH_3OH)] \quad (1)$$

$$[\text{Zn (SATPP)}] + H_2O \rightleftharpoons [\text{Zn (SATPP)}(H_2O)] \quad (2)$$

Scheme 3. The equilibria between four-coordinate and five-coordinate porphyrin complexes in solution.

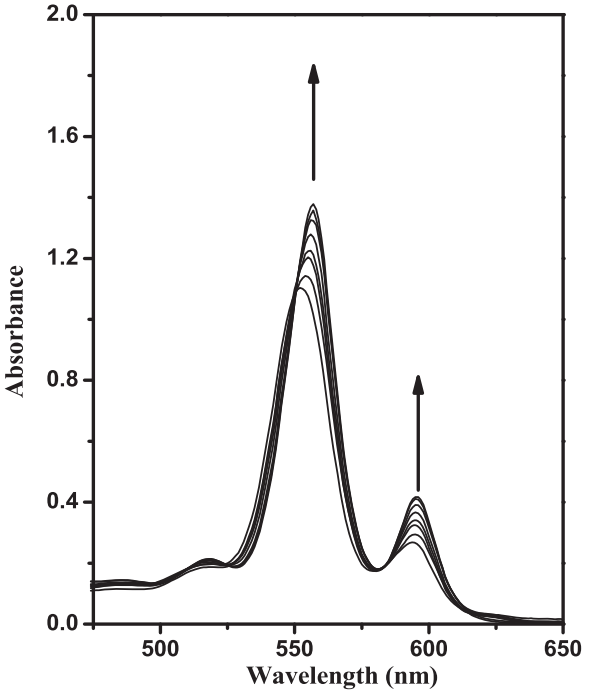

Figure 3. Spectral changes occurring upon titration of a [Zn(SATPP)] solution with methanol. Porphyrin concentration: 5.0×10^{-5} mol L^{-1}. Spectrum recorded at 25°C with dichloromethane as the solvent. In the titration, each step represents the following ligand concentrations (mol L^{-1}) increasing in the direction of the arrow: 0, 2.27×10^{-3}, 4.90×10^{-3}, 7.64×10^{-3}, 1.11×10^{-2}, 3.67×10^{-2}, 4.94×10^{-2}, and 9.88×10^{-2}. The absorbance intensities at 557 nm were used for the linear least-squares analysis.

The binding constant K for the equilibrium (1) can be measured by UV-Vis spectroscopy according to the method in the literature [18]. Titrations of [Zn(SATPP)] with methanol have been performed and shown in figure 3. The following double reciprocal relationship can be defined [19]:

$$\frac{1}{\Delta A} = \frac{1}{K\Delta A_\infty} \times \frac{1}{[CH_3OH]} + \frac{1}{\Delta A_\infty}, \quad (3)$$

where $1/\Delta A$ is the reciprocal of the change in absorbance observed after the addition of methanol to a [Zn(SATPP)] solution, ΔA_∞ is the reciprocal of the y-intercept obtained in equation (2) and yields the absorbance change observed at infinite ligand concentrations. $1/\Delta A$ is plotted *versus* the reciprocal of the added ligand concentration, 1/[L]. Linear least-squares analysis [20] is used to evaluate the slope and y-intercept of

the plotted data; a sample is given in figure S3. The obtained slope is 0.0156 which gives K for the equilibrium as 174 L mol^{-1}. Such binding constant is over 10 times larger than the corresponding value for [Zn(TPP)] [18], suggesting that intramolecular hydrogen-bonding significantly increases the binding ability of methanol to zinc in [Zn(SATPP)(CH_3OH)].

4. Conclusion

We have designed and synthesized a Schiff-base porphyrin complex [Zn(SATPP)(CH_3OH)] with double intramolecular hydrogen bonds. ^{1}H NMR spectra suggest that the binding of methanol to zinc is an equilibrium in solution. X-ray crystallography shows that phenol oxygen is involved in double hydrogen bonds. The structural result proves that such Schiff-base porphyrin is capable of forming an intramolecular hydrogen bond with a coordinated ligand. Such hydrogen bond increases the binding affinity of zinc to methanol. This new porphyrin species provides us a model to study hydrogen-bonding function in biological system. Further investigation is undergoing.

Supplementary material

Figures S1 and S2 display the full ^{1}H NMR spectra at different concentrations. Figure S3 gives the linear fit for equation (3). Tables S1–S6 give complete crystallographic details, atomic coordinates, bond distances and angles, anisotropic temperature factors, and fixed hydrogen atom positions. CCDC 801533 contains the supplementary crystallographic data. These data can be obtained free of charge *via* www.ccdc.cam.ac.uk/conts/retrieving.html or by application to The Director, CCDC, 12 Union Road, Cambridge CB2 1EZ, UK; Fax: (+44) 1223 336 033; E-mail: deposit@ccdc.cam.ac.uk.

Acknowledgments

This work was supported by the Natural Science Foundation of China (No. 20971093).

References

[1] J. Peisach. *Ann. N. Y. Acad. Sci.*, **244**, 187 (1975).
[2] (a) B.A. Springer, S.G. Sligar, J.S. Olson, G.N. Phillips Jr. *Chem. Rev.*, **94**, 699 (1994); (b) S. Adachi, S. Nagano, K. Ishimori, Y. Watanabe, I. Morishima, T. Egawa, T. Kitagawa, R. Makino. *Biochemistry*, **32**, 241 (1993); (c) K.D. Egeberg, B.A. Springer, S.A. Martinis, S.G. Sligar, D. Morikis, P.M. Champion. *Biochemistry*, **29**, 9783 (1990); (d) G.D. Depillis, S.M. Decatur, D. Barrick, S.G. Boxer. *J. Am. Chem. Soc.*, **116**, 6981 (1994).
[3] T.L. Poulos, B.C. Finzel, A.J. Howard. *J. Mol. Biol.*, **195**, 687 (1987).
[4] M.T. Fisher, S.G. Sligar. *J. Am. Chem. Soc.*, **107**, 5018 (1985).

[5] G.I. Berglund, G.H. Carlsson, A.T. Smith, H. Szöke, A. Henriksen, J. Hajdu. *Nature*, **417**, 463 (2002).
[6] M. Gajhede, D.J. Schuller, A. Henriksen, A.T. Smith, T.L. Poulos. *Nat. Struct. Biol.*, **4**, 1032 (1997).
[7] (a) C. Hu, B.C. Noll, P.M.B. Piccoli, A.J. Schultz, C.E. Schulz, W.R. Scheidt. *J. Am. Chem. Soc.*, **130**, 3127 (2008); (b) C. Hu, B.C. Noll, C.E. Schulz, W.R. Scheidt. *Inorg. Chem.*, **47**, 8884 (2008).
[8] J.P. Collman. *Acc. Chem. Res.*, **10**, 265 (1977).
[9] G.E. Wuenschell, C. Tetreau, D. Lavalette, C.A. Reed. *J. Am. Chem. Soc.*, **114**, 3346 (1992).
[10] P.E. Goudriaan, X.-B. Jang, M. Kuil. *Eur. J. Org. Chem.*, 6079 (2008).
[11] G.M. Sheldrick. *SHELXL-97, Program for the Refinement of Crystal Structure*, University of Göttingen, Germany (1997).
[12] J. Nakazawa, M. Mizuki, J. Hagiwara, Y. Shimazaki, F. Tani, Y. Naruta. *Bull. Chem. Soc. Japan*, **79**, 1431 (2006).
[13] M.O. Senge, I. Bischoff. *Eur. J. Org. Chem.*, 1735 (2001).
[14] (a) K. Ogawa, Y. Kasahara, Y. Ohtani, J. Harada. *J. Am. Chem. Soc.*, **120**, 7105 (1998); (b) M.R. Salata, T.J. Marks. *J. Am. Chem. Soc.*, **130**, 12 (2008).
[15] (a) G.O. Dudek, E.P. Dudek. *J. Am. Chem. Soc.*, **88**, 2407 (1966); (b) R.S. Becker, W.F. Richey. *J. Am. Chem. Soc.*, **89**, 1298 (1967); (c) E. Hadjoudis, F. Milia, J. Seliger, R. Blinc, V. Zagar. *Chem. Phys.*, **47**, 105 (1980); (d) T. Inabe, S. Gautier-Luneau, N. Hoshino, K. Okaniwa, H. Okamoto, T. Mitani, U. Nagashima, Y. Maruyama. *Bull. Chem. Soc. Japan*, **64**, 801 (1991); (e) T. Inabe, I. Luneau, T. Mitani, Y. Maruyama, S. Takeda. *Bull. Chem. Soc. Japan*, **67**, 612 (1994); (f) K. Wozniak, H. He, J. Klinowski, W. Jones, T. Dziembowska, E. Grech. *J. Chem. Soc., Faraday Trans.*, **91**, 3926 (1995); (g) A.R. Katritzky, I. Ghiviriga, P. Leeming, F. Soti. *Magn. Reson. Chem.*, **34**, 518 (1996); (h) S.H. Alarcón, A.C. Olivieri, A. Nordon, R.K. Harris. *J. Chem. Soc., Perkin Trans.* **2**, 2293 (1996); (i) T. Sekikawa, T. Kobayashi, T. Inabe. *J. Phys. Chem. A*, **101**, 644 (1997).
[16] A. Makal, W. Schilf, B. Kamieński, A. Szady-Chelmienieck, E. Grech, K. Woźniak. *Dalton Trans.* (2010) view online, DOI: 10.1039/C0DT00298D.
[17] C.J. Medforth. In *The Porphyrin Handbook*, K. Kadish, K. Smith, R. Guilard (Eds), Vol. 5, Academic Press, New York (2000).
[18] J.V. Nardo, J.H. Dawson. *Inorg. Chim. Acta*, **123**, 9 (1986).
[19] J.V. Nardo, J.H. Dawson. *Spectrosc. Int. J.*, **2**, 326 (1983).
[20] N.R. Draper, H. Smith. *Applied Regression Analysis*, 2nd Edn, Wiley, New York (1981).